IIETA International Information and Engineering Technology Association
Advancing the World of Information and Engineering

Traitement du Signal
Vol. 39, No. 2, April, 2022, pp. 737-744
Journal homepage: http://iieta.org/journals/ts

Orchard Boumans Algorithm and MRF Approach Based on Full Threshold Segmentation for Dental X-Ray Images

Vikram Rajpoot[1*], Rahul Dubey[2], Safdar Sardar Khan[3], Saumil Maheshwari[1], Abhishek Dixit[1], Arpit Deo[3], Nitika Vats Doohan[3]

[1] Department of Information Technology, Madhav Institute of Technology & Science, Gwalior 474005, India
[2] Department of Electronics Engineering, Madhav Institute of Technology & Science, Gwalior 474005, India
[3] Department of Computer Science & Engineering, Medi-Caps University, Indore 453331, India

Corresponding Author Email: rahul@mitsgwalior.in

https://doi.org/10.18280/ts.390239

Received: 11 March 2022
Accepted: 15 April 2022

Keywords:
thresholding, segmentation, specificity, X-ray, Markov random field, orchard humans, gaussian mixture model (GMM), grabCut method

ABSTRACT

Dental X-ray segmentation uses different image processing (IP) methods helpful in diagnosing medical applications, clinical purposes & in real-time. These methods aim to define the segmentation of various tooth structures in dental X-rays which are utilized to identify caries, tooth fractures, treatment of root canals, periodontal diseases, etc. The manual segmentation of Dental X-ray images for medical diagnosis is very complex and time-consuming from broad clinical databases. Orchard & Bouman is a color quantization approach used to evaluate a successful cluster division using an eigenvector of a color covariance matrix. It is repeated until the number of target clusters is reached. It is optimal for large clusters with Gaussian distributions to integrate different types of information on probabilism and spatial constraint by iteratively upgrading the later probability of the proposed model. Results of segmentation are achieved when iteration converges. Testing the proposed model's effectiveness will involve texture, distance sensing, and nature images. Experimental results show that our model achieves a higher segmentation precision with approximately 78.98 PSNR than MRF models based on pixels or regions.

1. INTRODUCTION

Radiographic images are important sources of information for the diagnosis of dentistry. Radiography is a photographic record of an image produced through an object by passing an X-ray source. X-ray images were utilized in dentistry to test mouth conditions in jaws, teeth, gums, & bone structure. Dentists could not detect most dental issues before they get serious without X-rays. Thus, radiographic examination supports the dentist in detecting reason and delineating the best treatment plan for the patient at an early stage [1]. A variety of advances in the image processing (IP) of medication may be seen in the literature for healthy diagnosis and treatments, as the latest developments in IP are emerging. The applications of IP in the medical field are growing today. In medical IP, segmentation is an important task. Segmentation means that an image is divided into different parts by process. The pixels of this type are of the same kind. In the proposed study, we concentrate on tooth segmentation based on thresholds as well as associated component analysis from periapical images. We achieve the extracted area of an item as part of the segmentation process. Every segmented tooth displays the region of interest (ROI) with distinct characteristics utilized in the following identification steps. Automated segmentation of teeth on X-ray images is challenging, firstly due to the poor quality of x-rays, and secondly due to segmentation costs. One of the essential data for dental biometrics is the radiograph images. Common three forms of dental X-ray images are Bitewing, panoramic dental images & periapical images.

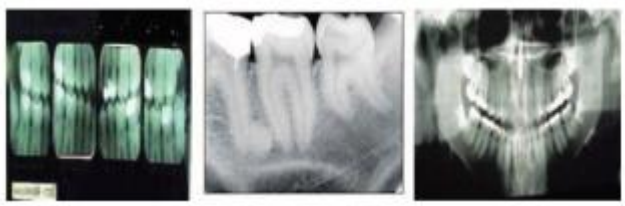

(A) (B) (C)

Figure 1. (A) Bitewing dental images (B) Periapical dental image (C) Panoramic dental images

Lower and Upper teeth are concentrated in bite-wings-rays. Periapical X-ray presents a whole tooth structure from lower jaw to upper jaw coronary. Panoramic X-ray detects teeth dependent upon lower and upper jawbones and offers more data on the teeth [2]. For identification purposes, it can be used as a good function. The detection of separate identities with dental X-ray images has gained much interest by improving the digitalization of stomatology images as well as advancing computer IP technology. It is now one of the hot research topics of human identification. To identify teeth with dental X-ray images, teeth of interest must be segmented and their entire contour extracted and characteristics then extracted. The values of these functions can then be collected from specific teeth for identification purposes. The classification approach depends heavily on the segmentation algorithm included in this case. The dental X-ray IP and the reconstruction of contours and structures lost morphology in images of injured tissues are therefore important tasks for biomedical

applications. It is beneficial to have an exact and reliable segmentation algorithm for processing dental X-ray images [3]. Estimated structural data on pre-damaged tissue may be used for various uses like 3D tissue diagnosis & restoration.

(A) (B)

Figure 2. (A) 3D printed skull cap to repair of cranial damage. (B) A proximal surface dental cavity in restoration needs

The application of 3D printing, CAD or CAM technologies to reconstruct hard tissues, make scaffolds and organ 3D models, as well as make analogs by a CAD-based design and manufacturing is a developing field in biomedical engineering, as shown in Figure 2. The leading information sources for CAD or CAM-based tissue engineering are 3D images by non-destructive imagery like magnetic resonance imaging (MRI)as well as computed tomography (CT) [4].

1.1 Digital dental radiograph (X-rays)

Dental Radiographs (X-rays) are a variety of teeth as well as mouth pictures. Radiation is like visible light, a source of electromagnetic radiation. These are stronger as well as may infiltrate the body to form a film frame. Dense structures (for example, metal restorations or silver fillings) block the majority of photons also appear white on developed film. Air-containing structures appear black in the film while teeth, tissue & liquid seem like gray shades. Dental X-rays will help you to find teeth, mouth & jaw issues. Dental x-ray images may show cavities, dental structures concealed (for example wisdom teeth) and no visual loss. These are very effective to identify the early decay of the teeth.

Just half the radiation dose is required in comparison with conventional X-rays to obtain equivalent dental X-rays. Dentists only have to wait a few seconds before the film image is shown. They need no time for film development. In common, digital dental X-rays inpatient record have good image quality than traditional dental X-rays, so that dentists may immediately take any other image when a developed image is of no better quality. Digital dental X-rays are utilized regularly, mainly because of their advantages in speed, storage as well as image quality [5].

1.2 Types of dental radiographs

A very general type of radiography in dentistry is intraoral X-rays. bone, Tooth& supporting tissues of the mouth are highly detailed. These X-rays enable dentists:

- Find cavities
- Look at tooth roots
- Check health of bony area around the tooth
- Help diagnose periodontal disease
- See status of developing teeth

(1) Bitewing X-ray the back of the teeth is illustrated in Figure 1 (A). On either side of the mouth, dentists take ½ bite-wing X-rays. Lower and upper molars (back teeth), as well as bicuspids (teeth before molars), are shown in each of x-rays. These X-rays are known as "bite-wings," as you drag on a wing-shaped frame holding film while X-ray is being reserved. These X-rays help dentists to deteriorate among their back teeth. Bitewing is displayed in Figure 3(A).

(2) Periapical X-ray Only one or two teeth are highlighted at a time. The whole length of each tooth is shown in Figure 1(B) from crown to root. This was used to determine caries in the tooth, as it allows a dentist to view both the entire tooth and surrounding teeth illustrated in Figure 3(B).

(3) Occlusal View emphasize tooth improvement. Every X-ray reveals an upper or lower jaw with almost the complete arch of teeth. The film lies on teeth's bite surface as mentioned in Figure 3(C).

(4) Panoramic View Panoramic X-rays show the whole teeth structure with jaws and teeth in a single view as mentioned in Figure 3(D). These types of X-rays are used to detect different infections or problems present in teeth such as cysts, fractures, tumors, impacted teeth, and dental caries, etc. [6].

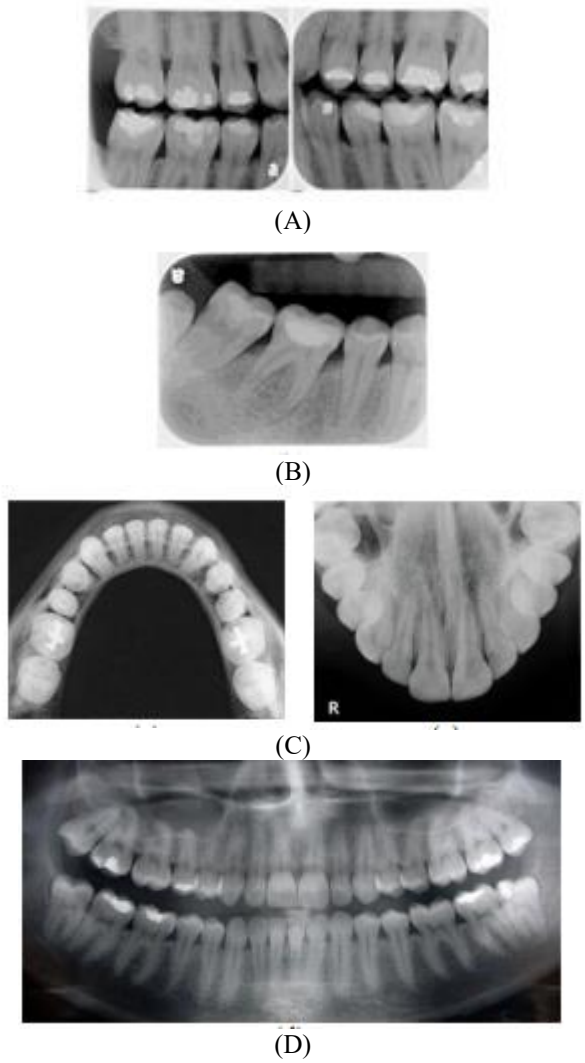

(A)

(B)

(C)

(D)

Figure 3. (A) Bitewing view (B) Periapical view (C) Occlusal view (D) Panoramic view

3-D models of the tooth-alveolar bone complex are needed to prepare treatment and simulation of computer-aided orthodontics. Tooth segmentation and alveolar bones by CT images is a crucial step in restoring their models. As alveolar

bone is less used in traditional orthodontic procedures and can cause adverse side effects, preceding studies were generally concerned with dental reconstruction & segmentation as well as failed to take into account alveolar bone. In the research, Gan et al. suggested using dental CT images for 3-D models reconstruction for both tooth & alveolar bone segmentation. Next, a planned technique was used to remove related tooth region& alveolar bone by CT images using a global convex level set model [7].

Wu et al. discusses using a set of orthodontic assessment criteria to achieve better patient results by the dentists. A new way of helping the dentist achieve a consistent analysis of these criteria is proposed in this report. It may be categorized into 4 phases: model training, IP, tooth segmentation, and orthodontic parameter assessment. This method is based on panoramic dental radiography. The image is normalized & improved first. The model learning phase consists of shape & image model training and weight training. First, tooth contours are automatically segmented energy-minimized. In the middle, orthodontic criteria are automatically evaluated. Experimental results show an average range between 4.17 and 6.03, 0.87, 0.90 and 2.58 and 3.12 for coefficients for dice similitudes & average qualitative scores, respectively. The orthodontic test is also very similar to an orthodontic assessment. For helping dentists achieve an objective assessment, the proposed method would provide accurate & consistent measurements [8].

Thresholding is a way of segmenting an image into a foreground and background according to a fixed constant value called a threshold. Image segmentation based on a constant threshold leads to unsatisfactory results with dental X-ray images because of the uneven pixel intensity distribution. Razali et al. proposed an adaptive thresholding method to attain promising segmentation results in dental X-ray images. Mean, Median, Midgrey, Niblack, and OTSU thresholding methods are utilized to delineate the acceptable range of threshold values for segmenting X-ray images. Experimental results showed that the Median method consistently achieves the best range of threshold values between 57 and 86 in grayscale [9].

Many pathologies arise in dental studies, such as dental caries or jaw cysts. The dental defects were assessed by X-ray analysis. The standard method of screening patients with easy imaging and reduced patient exposure is panoramic radiography/orthopantomography (OPG). The panoramic images obtained from this device were taken from the sound of dental caries that were implanted during its creation. The application of computer-assisted IP algorithms on dental panoramic images can improve identification & dental caries classification & some additional maxillofacial pathologies. Veena et al. introduced different dental abnormalities detection IP algorithms [10].

Hatvani et al. proposed two CNN architectures— a sub-pixel n/w, and a so-called U-net — to increase the resolution of 2D cone-beam CT ex vivo teeth image slices. To this end, a training package of 4 structurally different teeth was supported for 13 teeth 5680 cross-section slices as well as a test set of 1824 slices. For comparison, two existing super-resolution methods based on reconstruction using' 2-norm' and total variation regularization were utilized. Different measures (structure similarity index, peak signal-to-noise, and additional objective measures to approximate human perception), including subsequent analysis based on image segmentation were used for tests to be analyzed. Micro-CT images have been used as a basis for the assessment. The results indicate superior dental CT images of the proposed CNN-based approach with reconstruction methods that allow an excellent finding of medically important aspects, like size, shape/root canal curvature [11].

Janardanan and Logeswaran suggest that Image processing is a robust tool aiding medical and forensic research. This paper covers a systematic review of dental image analysis applied to forensic odontology. Interpretation of medical images relies heavily on the presence of people as well as the human perception of details found therein, and interpretation of fine details in different contrasting circumstances of a medical image is a challenge because standard x-rays by a regular acquisition device can only be of average quality [12]. Many standard scientific methods developed by researchers' scholars & software developers in order to address this form of deficiency in a medical radiograph were investigated to mitigate possible error in human estimation based solely on human visual perception of correct diagnosis & treatment.

In dentistry, radiological examinations assist specialists with the structures of teeth with the aim of screening embedded teeth, bone abnormalities, tumors, cysts, fractures, infections, and time-sensitive issues. Based on expert's views alone, variations in interpretation can sometimes result, which can inevitably delay treatment. Although no fully automatic diagnostic tools are planned yet, image pattern recognition has developed to aid decision making, primarily from identifying teeth & components in X-ray images, as concluded by Jader et al. For at least the last two decades, threshold detection has been subject to research & relies mainly on local methods. This paper suggests investigating, for instance, a detailed learning technique to segment teeth according to a different direction. This is their first device to detect each tooth & segment it in panoramic X-ray images to the greatest extent possible [13].

Singh and Sehgal propose a technique to classify panoramic dental images. The proposed work is divided into four stages namely pre-processing, segmentation, numbering and classification. Then the preprocessed images are segmented using fuzzy c-mean clustering, then vertical integral projection are applied to extract single tooth image [14].

Kumar et al. proposes a Tangent Gaussian kernel Fuzzy C-Means algorithm to increase the effectiveness of other traditional methods. Authors Identified that the current method is less sensitive to noise with robustness. Cluster validity computation is achieved using Davis-Bouldin, Segmentation Accuracy, PBM and Mean absolute Error (MAE) [15].

2. METHODOLOGY USED

2.1 Segmentation

In segmentation procedure, dental X-ray images consist of different regions, backgrounds, teeth and bone structure areas around the teeth. Mostly bright grayscale values indicate the tooth region, the middle range of grey values shows the bone region and the background always maps the dark region. The major objective of the proposed segmentation algorithm is to find the shape of every individual tooth and based on that detection of abnormal tooth present in dental X-ray images & segmentation is improved by using morphological operations [16].

2.2 Thresholding

After minimizing the unwanted noise from the images, we apply the threshold process to divide the teeth from the background. A binary image is produced after applying thresholding that renders image examination simpler. In most of the dental images, we observe the occurrence of a shading consequence that manifests like the rise of image intensity. Therefore, it is not preferable to use only a single threshold value because information pixels may be lost. Upon reducing noise, histograph of filtered image includes the percentage of the object pixels below the level of a certain grayscale.

The threshold is easy as well as suitable for images containing solid objects with a uniform background brightness. An adequate threshold value is necessary for the success of thresholding [17]. Global thresholding which is based on the assumption that the image has a bimodal histogram and, therefore, the object can be extracted from the background by a simple operation that compares image values with a threshold value. This is a well-established method and found uses in medical images dominantly [18]. To simplify & maintain generality, one global single threshold T is presumed to be utilized to divide an image into 2 different regions: 0= foreground& 1= background. The following can be described as a predicate function P:

$$P(R_0) = true, if \forall x \in R_0, f(x) \geq T \quad (1)$$

$$P(R_1) = true, if \forall x \in R_1, f(x) < T \quad (2)$$

The pixels 1 belong to the foreground as well as pixels 0 to a background of images. The consequence of the international thresholding method is shown in Figure 7.

$$g(x) = \begin{cases} r_0 \; iff(x) \geq T \\ r_1 \;\; otherwise \end{cases} \quad (3)$$

2.3 Median filtering

Enhancement is used to improve the visualization of image properties clearly. The enhancement depends on the type of process like extract or restores image information. The domain of application decides the type of enhancement technique. Basically, filters used to remove noise from images and present images as sketchy manner. There is a lot of filters available, here the median filter used to reduce the noise. It is better than the mean filter in preserving high-frequency details in the image. Median filter based on numerical values, mid-value is fixed as median m, and there is a two range below m and greater than m. At every pixel location, the median filter needs ordering neighborhood values [19].

$$(x, y) = median\left(D_i(x, y)\right) \quad (4)$$

2.4 Target tooth image obtainment via grabCut

Graph Cut [20] also maps image in a network with n+ 2 nodes with n pixels. It is an undirected graph G= (V, E), where V is a finite group of nodes which are non-empty, as well as E, is edge set of disordered node pair. 2 novel nodes are S & sink point T, representing the convergence of target pixel and background pixel. Aside from interconnections between the image pixels, the source point S is connected to all target nodes as well as the sink point T is connected to all background nodes. And β = V − S, T = β1, β2,…, βn,…, βN, βn ∈ 0, 1, which is vector demonstrating value of every pixel, Background area marked as 0 as shown in Figs, target area marked as 1. 10a and b. Then, the n/w model is cut to get the minimum n/w model reduction, which is minimum energy value, to obtain the result of segmentation as shown in Figures 10c & d.

A new version of Graph Cuts [21] is the Grab Cut algorithm. As a segmentation basis, GrabCut utilizes the image's structure as well as boundary information, thus reducing user interaction. An image in Red, Green, Blue (RGB) color space is working too, for distribution of background & front pixels is described using a Gaussian mixture model (GMM) rather than the histogram. Front, as well as background areas, are equivalent to a GMM of full covariance composed of K (usually K= 5). To enable implementation of GMM, a new vector k = k1, k2,…,kn,…, kN is presented & kn∈ 1, …, K denotes Gauss component corresponding to the nth pixel. Every pixel is in front as well as background GMM up to βn ∈ 0, 1; thus pixel segmentation may be done by marking of pixels, as well as best pixel label can be found in optimum segmentation of the image. Researchers found that the network's maximum flow is min-cut. Therefore, by minimizing energy function whole segmentation procedure may be accomplished. Through the GMM solving energy minimization model, segmentation accuracy is effectively improved. Gibbs energy utilized to segmentation is

$$E\left(\underline{\beta}, k, \underline{\theta}, z\right) = U\left(\underline{\beta}, k, \underline{\theta}, z\right) + V\left(\underline{\beta}, z\right) \quad (5)$$

1st portion of energy function U is data term

$$U\left(\underline{\beta}, k, \underline{\theta}, z\right) = \sum_n D(\beta_n, k_n, \theta, z_n) \quad (6)$$

$$U\left(\underline{\beta}, k, \underline{\theta}, z\right) = -\log p\left(z, \beta_n, k_n, \underline{\theta}\right) - \log \pi(\beta_n, k_n) \quad (7)$$

p(•) is distribution of Gaussian probability, and π (•) means the coefficient of a mixture, hence

$$\begin{gathered} D\left(\beta_n, k_n, \underline{\theta}, z_n\right) = -\log \pi\left(\beta_n, k_n\right) + \\ \frac{1}{2}\log det \sum(\beta_n, k_n) + \frac{1}{2}[z_n - \\ \mu(\beta_n, k_n)]^T \sum(\beta_n, k_n)^{-1} [z_n - \mu(\beta_n, k_n)] \end{gathered} \quad (8)$$

θ is GMM parameter

$$\begin{gathered} \theta = \Big\{\pi(\beta, k), \mu(\beta, k), \sum(\beta, k), \beta = \{0,1\}, k \\ = \{1,2, \ldots \ldots, k\}\Big\} \end{gathered} \quad (9)$$

The proportion of every other Gaussian distribution of probabilities, mean as well as covariance is here π, β, k, μ β, k & ∑ β, k. 2ndportion of energy function V is a smooth term

$$V(\beta, z) = \gamma \sum_{(m,n) \in C} [\beta_n \neq \beta_m] exp - a z_m - z_n^2 \quad (10)$$

The greater the difference, the less energy between adjacent pixels. Here C represents all adjacent pixel pairs. About has 2 ways to ensure foreground & background, (i) interact manually by users and (ii) mask over. 2nd method is to reduce and improve the efficiency of iterations. Objective dental

image with mask GrabCut. The experiments also show that the GrabCut target tooth image needs nearly one iteration to be segmented using a mask.

3. PROPOSED METHODOLOGY

3.1 Orchard and bouman

Orchard & Bouman is a technique of color quantization that utilizes color covariance matrix eigenvector to identify good cluster divisions. The algorithm begins in a single cluster with all pixels. The cluster is then divided into two by the autonomous function of the covariance matrix as the split point. It then uses the covariance matrix's eigenvalues to choose which group is a candidate for the next section. This is achieved until optimal no. of clusters is reached. The solution with Gaussian distributions is optimal for large classes. A Gaussian mixture model (GMM) is a probabilistic model that assumes all the data points are generated from a mixture of a finite number of Gaussian distributions with unknown parameters. GMM can be considered as generalizing k-means clustering to incorporate information about the covariance structure of the data as well as the centers of the latent Gaussians [22]. Therefore, using the covariance matrix for deciding the number of clusters helps control the dominance of Gaussian distribution.

3.2 Markov random field (MRF)

An MRF image segmentation model is available to combine color & texture characteristics. In combinatorial optimization (simulated annealing), a conceptual framework builds on Bayesian evaluation. Segmentation is accomplished through pixels grouping into various pixel groups. The multi-variate Gaussian distributions reflect these groups. Gaussian parameters can be calculated using training data set and by input image. A parameter estimation technique with an EM algorithm is also proposed. Experimental outcomes are delivered to show both synthetic as well as natural color images of the performance of our method.

In the field of image segmentation (IS), MRF has been very attractive. The pixels and regions may form his basic unit. The advantages & disadvantages of such pixel or regionally based MRF models are their own. Firstly, the proposed model combines advantages of the model pixel and regionally based MRF by breaking down probability function into the product of pixel probability function as well as regional probability function. In order to combine various types of information about probability & spatial constraint, a theory probabilistic inference is established by iteratively updating the resulting probability of the proposed model. When iteration converges, segmentation results may be achieved. The efficiency of the proposed model is tested by exture, remote sensing as well as nature images. Test results show that the segmentation accuracy of our model is greater than that of pixel or regionally based MRF model.

3.3 Proposed algorithm

1. First, we take a dental X-Ray image from the dataset.
2. The image to be segmented is a grey value at pixel denotes threshold. In the image to be segmented, min & max respectively are minimum & maximum pixel grey scales.
3. Apply binarization to convert image in binary and find the accurate result of segmentation.
4. Create a target tooth mask on the binary image. Here we marked two tooth images in red box completely.
5. Apply median filtering to remove noise from the image.
6. Target tooth image obtained by grab cut method. Grab Cut algorithm is passed out to find an image that once has an outline of a target tooth image.
7. Instead of a histogram, GMM is used to describe foreground & background pixel distribution.
8. Apply orchard Youmans. Orchard Youmans algorithm applied to segment image.
9. Markov random field (MRF). MRF has been actively used in the image-processing community for modeling spatial correlations.
10. Performance analysis calculates the value of PSNR and MSE.
11. Exit

All these stages are mentioned in Figure 4.

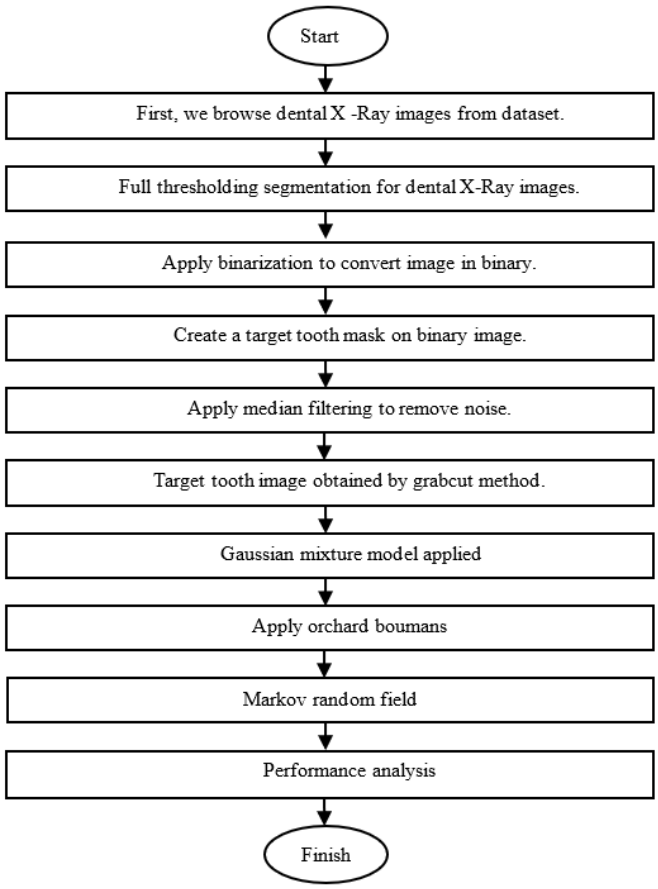

Figure 4. Flow chart of proposed work

4. RESULT AND DISCUSSION

The algorithm is simulated on MATLABR18a using the IP toolbox. In this operation, this algorithm is matched with dissimilar algorithms. The output of all the overhead mentioned techniques is compared on the foundation of their corresponding accuracy values and the output. First, we ran this code and obtained Figure 5 menu bar type.

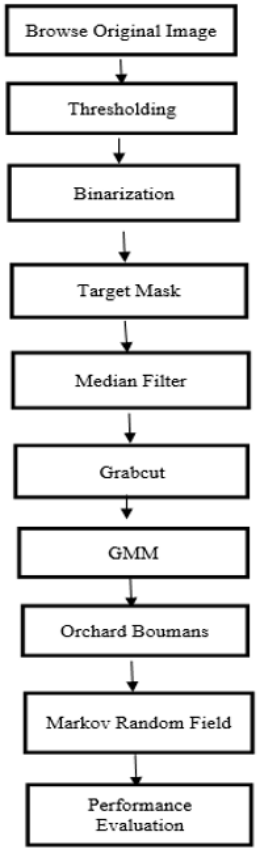

Figure 5. 10 steps in this menu bar

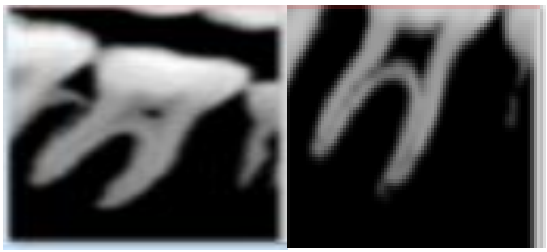

Figure 6. First, we browse the dental X-ray image from the dataset

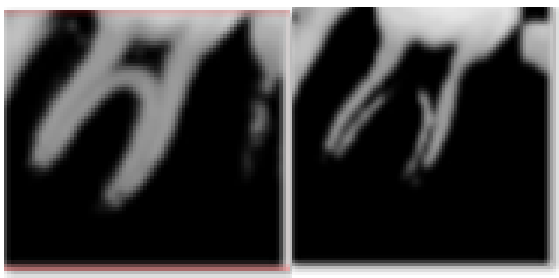

Figure 7. Full thresholding segmentation for dental X-ray images

First, Browse the dental X-Ray images from the dataset, as illustrated in Figure 6. Full Thresholding is applied on X-Ray images; the result is mentioned in Figure 7. Then images are converted into Binary mentioned in Figure 8. After that, a target tooth mask is applied to the binary image, as shown in Figure 9. Noises are removed using a median filter, as shown in Figure 10. Then GrabCut is applied to obtain the target tooth image given in Figure 11. The results of the Gaussian Mixture model are illustrated in Figure 12.

Figure 8. Apply binarization to convert image in binary

Figure 9. Create a target tooth mask on a binary image

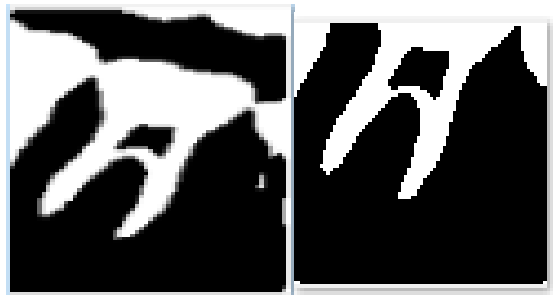

Figure 10. Apply median filtering to remove noise

Figure 11. Target tooth image obtained by grabCut method

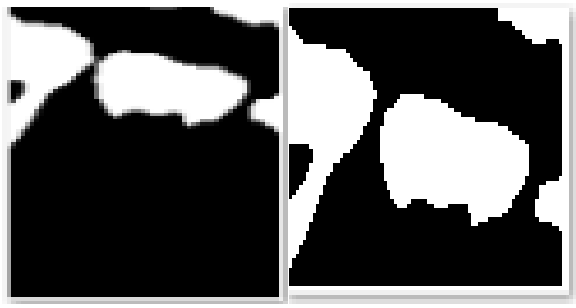

Figure 12. Gaussian mixture model applied

Results of Orchard Voumans and Markov Random field are mentioned in Figure 13 and Figure 14 respectively.

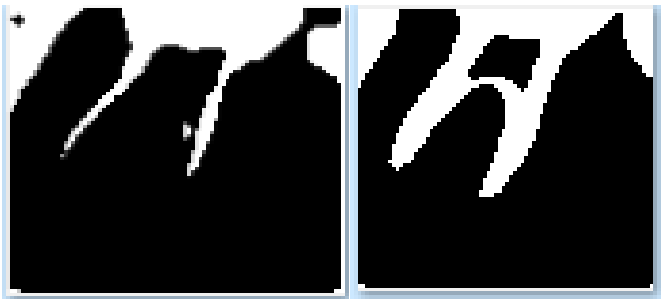

Figure 13. Apply orchard Youmans

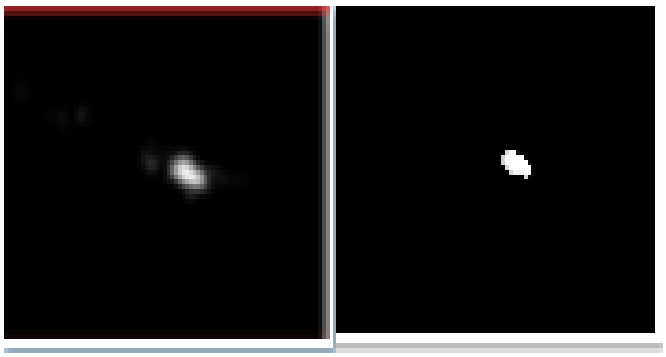

Figure 14. Markov random field (MRF)

Table 1 indicates the performances of Base PSNR and proposed PSNR. Figure 15 is the Column graph comparative representation. Performances of Base MSE and proposed MSE are discussed in Table 2. Figure 16 is the Column graph graphical of it. Table 1 indicates the comparison between the PSNR values of the proposed algorithm with the algorithm considered as a base algorithm.

In contrast, Table 2 indicates the comparison between the proposed algorithm's mean square error values with the algorithm considered a base algorithm. For Teeth 1, the base PSNR is 64.3862, while for the proposed algorithm, it is 74.3436; similar results are there for teeth 2 and teeth 3. For Teeth 1 base mean square error was 0.9585, which was higher than the proposed algorithm in which the mean square error is 0.5768; similar results are there for teeth 2 and teeth 3, respectively. The same results have been reflected and plotted using the bar chart between PSNR value of the base and the proposed algorithm in Figure 15, and for MSE, it is plotted in Figure 16.

Table 1. Comparison of base PSNR and proposed PSNR

Image Name	Base PSNR	Proposed PSNR
Teeth1.jpg	64.3862	74.3436
Teeth2.jpg	42.6424	78.9854
Teeth3.jpg	47.7988	73.6453

Table 2. Comparison of base MSE & propose MSE

Image Name	Base MSE	Proposed MSE
Teeth1.jpg	0.9585	0.5768
Teeth2.jpg	0.8746	0.7337
Teeth3.jpg	0.8383	0.6574

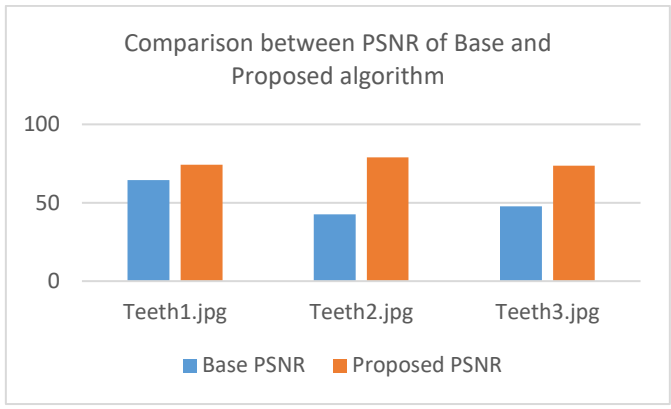

Figure 15. Column graph comparison of base PSNR and propose PSNR

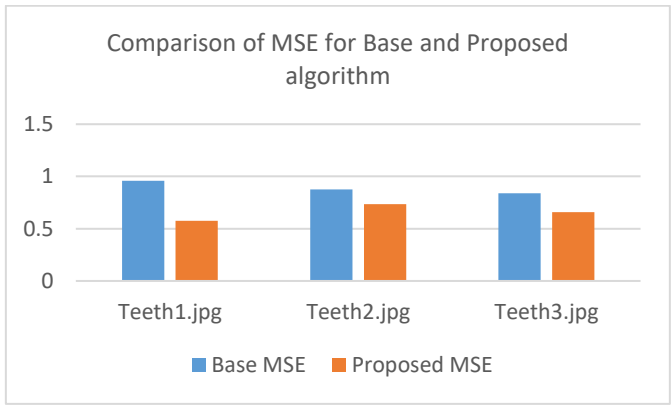

Figure 16. Column graph comparison of base MSE and propose MSE

5. CONCLUSION

The use of image processing is found extensively in the field of medical imaging. The manual segmentation of Dental X-ray images for medical diagnosis is very complex and time-consuming, from broad clinical databases. This paper proposed an Orchard Boumans Algorithm and MRF Approach Based on Full Threshold Segmentation for Dental X-Ray Images. Orchard & Bouman is a color quantization approach used to evaluate a successful cluster division using an eigenvector of a color covariance matrix. It is repeated until the number of target cluster is reached. It is an optimal way for large clusters with Gaussian distributions to integrate different types of information on probabilism, and spatial constraint by iteratively upgrading later probability of the proposed model. Experimental results show that our model may achieve a higher segmentation precision than MRF models based on pixels or on regions.

ACKNOWLEDGEMENT

We would like to acknowledge Madhav Institute of Technology and Science, Gwalior for providing the opportunity to work on this problem and providing the necessary resources. Further, we declare this is a part of academic progress and no funding is issued for this work.

REFERENCES

[1] Silva, G., Oliveira, L., Pithon, M. (2018). Automatic segmenting teeth in X-ray images: Trends, a novel data set, benchmarking and future perspectives. Expert Systems with Applications, 107: 15-31. https://doi.org/10.1016/j.eswa.2018.04.001

[2] Chandran, V., Nizar, G.S., Simon, P. (2019). Segmentation of dental radiograph images. In Proceedings of the Third International Conference on Advanced Informatics for Computing Research, 1-5. https://doi.org/10.1145/3339311.3339344

[3] Mao, J., Wang, K., Hu, Y., Sheng, W., Feng, Q. (2018). GrabCut algorithm for dental X-ray images based on full threshold segmentation. IET Image Processing, 12(12): 2330-2335.

[4] Lashgari, M., Shahmoradi, M., Rabbani, H., Swain, M. (2018). Missing surface estimation based on modified tikhonov regularization: Application for destructed dental tissue. IEEE Transactions on Image Processing, 27(5): 2433-2446. https://doi.org/10.1109/TIP.2018.2800289

[5] Jain, K.R., Chauhan, N.C. (2015). Efficacy of digital image processing techniques in intra oral dentistry. International Journal of Current Engineering and Scientific Research (IJCESR), 2(2): 2394-0697.

[6] Solanki, A.J., Mahant, P.M. (2017). A review on dental radiographic images. International Journal of Engineering Research and Application, 7(7): 49-53.

[7] Gan, Y., Xia, Z., Xiong, J., Li, G., Zhao, Q. (2017). Tooth and alveolar bone segmentation from dental computed tomography images. IEEE Journal of Biomedical and Health Informatics, 22(1): 196-204. https://doi.org/10.1109/JBHI.2017.2709406

[8] Wu, C.H., Tsai, W.H., Chen, Y.H., Liu, J.K., Sun, Y.N. (2017). Model-based orthodontic assessments for dental panoramic radiographs. IEEE Journal of Biomedical and Health Informatics, 22(2): 545-551. https://doi.org/10.1109/JBHI.2017.2660527

[9] Razali, M.R.M., Ismail, W., Ahmad, N.S., Bahari, M., Zaki, Z.M., Radman, A. (2017). An adaptive thresholding method for segmenting dental X-ray images. Journal of Telecommunication, Electronic and Computer Engineering.

[10] Veena Divya, K., Jatti, A., Joshi, R., Deepu Krishna, S. (2017). Characterization of dental pathologies using digital panoramic X-ray images based on texture analysis. 2017 39th Annual International Conference of the IEEE Engineering in Medicine and Biology Society (EMBC), pp. 592-595. https://doi.org/10.1109/EMBC.2017.8036894

[11] Jatti, A., Joshi, R. (2017). Characterization of dental pathologies using digital panoramic X-ray images based on texture analysis. In 2017 39th Annual International Conference of the IEEE Engineering in Medicine and Biology Society (EMBC), pp. 592-595. https://doi.org/10.1109/EMBC.2017.8036894

[12] Janardanan, R.P., Logeswaran, R. (2018). Recent image processing techniques in forensic odontology-a systematic review. Biomedical Journal of Scientific & Technical Research, 2(5): 1-6. https://doi.org/10.26717/BJSTR.2018.2.000825

[13] Jader, G., Fontineli, J., Ruiz, M., Abdalla, K., Pithon, M., Oliveira, L. (2018). Deep instance segmentation of teeth in panoramic X-ray images. In 2018 31st SIBGRAPI Conference on Graphics, Patterns and Images (SIBGRAPI), pp. 400-407. https://doi.org/10.1109/SIBGRAPI.2018.00058

[14] Singh, P., Sehgal, P. (2020). Numbering and classification of panoramic dental images using 6-layer convolutional neural network. Pattern Recognition and Image Analysis, 30(1): 125-133. https://doi.org/10.1134/S1054661820010149

[15] Kumar, A., Bhadauria, H.S., Singh, A. (2020). Semi-supervised OTSU based hyperbolic tangent Gaussian kernel fuzzy C-mean clustering for dental radiographs segmentation. Multimedia Tools and Applications, 79(3): 2745-2768. https://doi.org/10.1007/s11042-019-08268-8

[16] Anuj, K., Bhadauria, H.S., Nitin, K. (2018). Segmentation of periapical dental X-ray images by applying morphological operations. International Journal of Engineering Research in Computer Science and Engineering (IJERCSE), 5(2).

[17] Rad, A.E., Mohd Rahim, M.S., Rehman, A., Altameem, A., Saba, T. (2013). Evaluation of current dental radiographs segmentation approaches in computer-aided applications. IETE Technical Review, 30(3): 210-222. https://doi.org/10.4103/0256-4602.113498

[18] Rogowska, J. (2000). Overview and fundamentals of medical image segmentation. Handbook of Medical Imaging, Processing and Analysis, 69-85.

[19] Thamilarasi, V., Roselin, R. (2019). Automatic thresholding for segmentation in chest X-ray images based on green channel using mean and standard deviation. International Journal of Innovative Technology and Exploring Engineering (IJITEE), 8(8): 695-699.

[20] Boykov, Y.Y., Jolly, M.P. (2001). Interactive graph cuts for optimal boundary & region segmentation of objects in ND images. In Proceedings Eighth IEEE international Conference on Computer Vision. ICCV 2001, 1: 105-112. https://doi.org/10.1109/ICCV.2001.937505

[21] Rother, C., Kolmogorov, V., Blake, A. (2004). "GrabCut" interactive foreground extraction using iterated graph cuts. ACM Transactions on Graphics (TOG), 23(3): 309-314. https://doi.org/10.1145/1015706.1015720

[22] McNicholas, P.D. (2016). Mixture Model-Based Classification. Chapman and Hall/CRC.